A Murine Living Skin Equivalent Amenable to Live-Cell Imaging: Analysis of the Roles of Connexins in the Epidermis

Eve E. Kandyba[1], Malcolm B. Hodgins[1] and Patricia E. Martin[1]

Three-dimensional (3D) organotypic models are increasingly used to study the aspects of epidermal organisation and cutaneous wound-healing events. However, these are largely dependent on laborious histological analysis and immunohistochemical approaches. Despite the large resource of transgenic and knockout mice harboring mutations relevant to skin disorders, few organotypic mouse skin models are available. We have developed a versatile *in vitro* 3D organotypic mouse skin equivalent that reflects epidermal organisation *in vivo*. The system is optically transparent and ideally suited to real-time analysis using a variety of integrated *in situ* imaging techniques. As a paradigm for coordination of cellular events, the epidermal gap junction network was investigated and the model displayed predominant connexin 43 (Cx43) expression in basal proliferating cells and Cx26 and Cx30 expression in differentiated keratinocytes. We show that attenuation of Cx43-mediated communication by a Cx mimetic peptide enhanced wound closure rates in keratinocyte monocultures and in the living skin equivalent system, emphasising the utility of the model to systematically unravel the molecular mechanisms underlying epidermal morphogenesis, assess promising therapeutic strategies, and reduce animal experimentation. Furthermore, we visualise epidermal regeneration following injury in real time, thereby facilitating avenues to explore distinctive modes of wound re-epithelialisation in a non-invasive manner.

Journal of Investigative Dermatology (2008) **128,** 1039–1049; doi:10.1038/sj.jid.5701125; published online 25 October 2007

INTRODUCTION

Three-dimensional (3D) organotypic skin models, primarily human based, provide insights into developmental skin biology and epidermal differentiation events (Parenteau *et al.*, 1992; Arita *et al.*, 2002; Harrison *et al.*, 2006). Complementary use of *in vivo* transgenic and knockout mouse resources enable analysis of cellular events concerning epidermal morphogenesis (Maestrini *et al.*, 1999; Bakirtis *et al.*, 2003) and homeostasis; however, few *in vitro* murine organotypic skin models exist. Those available often employ fibroblast-incorporated collagen supports or a dead de-epidermised dermis (Carroll and Moles, 2000; Ikuta *et al.*, 2006), which can impede the direct *in situ* visualisation of morphological events and require arduous histological processing.

To address this problem, we have developed a versatile and robust Transwell murine skin model, incorporating primary murine fibroblasts and keratinocytes, which once raised to the air–liquid interface (ALI), stratifies and differentiates to produce a 3D organotypic skin equivalent that possesses morphological and differentiation characteristics typical of those observed *in vivo*. The transparent nature of the Transwell semipermeable membranes permits visualisation of these complex morphological events in real time via an array of imaging techniques, negating the need for standard histological techniques, as epidermal differentiation events may be imaged *in situ* by whole-mount and 3D Z-stack reconstruction following single or dual-label indirect immunofluorescence. This versatile *in vitro* system provides the opportunity to examine aspects of integrated cellular behavior and enables one to functionally probe, image, and analyze the coordination of epidermal homeostasis. A paradigm for coordination of cellular activities is direct cell to cell communication via an integrated network of gap junctional intercellular communication channels.

With few exceptions, practically all animal cells *in vivo* are linked via gap junctions, intercellular channels that permit exchange of small molecules and ions below 1 kDa between neighboring cells. Connexins (Cxs), a family of highly conserved transmembrane proteins, are the constituent proteins of vertebrate gap junctions, and different Cxs can form channels of varying permeabilities and

[1]*Department of Biological and Biomedical Sciences, School of Life Sciences, Glasgow Caledonian University, Glasgow, UK*

Correspondence: Dr Patricia E. Martin, Department of Biological and Biomedical Sciences,School of Life Sciences, Glasgow Caledonian University, Glasgow G4 0BA, UK. E-mail: patricia.martin@gcal.ac.uk

Abbreviations: ALI, air–liquid interface; Cx, connexin; 3D, three dimensional; DAPI, 4,6-diamidino-2-phenylindole; DED, dead de-epidermised dermis; GJIC, gap junctional intercellular communication; siRNA, short interfering RNA

Received 19 February 2007; revised 21 August 2007; accepted 27 August 2007; published online 25 October 2007

functional properties that may reflect differing physiological requirements of cells in tissues and organs (see reviews by Evans and Martin, 2002; Laird, 2006). An elaborate gap junction network exists within the skin, where keratinocytes spatially express Cxs in specific and often overlapping patterns within the differentiating layers of the epidermis (Salomon *et al.*, 1994; Wiszniewski *et al.*, 2000; Di *et al.*, 2001a). The importance of Cxs in epidermal networks is highlighted by the increasing number of Cx mutations found to underlie genetically inherited skin disorders, particularly Cx26 (Maestrini *et al.*, 1999; Di *et al.*, 2001b; Richard *et al.*, 2002), Cx30 (Common *et al.*, 2002; Essenfelder *et al.*, 2004), Cx30.3 (Macari *et al.*, 2000), Cx31 (Richard *et al.*, 2000) and Cx43 (Kelly *et al.*, 2006; Vreeburg *et al.*, 2007). Furthermore, changes in Cx expression profiles are associated with wound healing events (Goliger and Paul, 1995; Mori *et al.*, 2006) and a variety of skin disorders including psoriasis (Labarthe *et al.*, 1998; Lucke *et al.*, 1999). Although the exact role of specific Cxs has yet to be fully determined, it is likely that gap junctions are required to coordinate keratinocyte proliferation, migration, and differentiation events during epidermal morphogenesis, and are emerging as therapeutic targets to improve wound healing (Qiu *et al.*, 2003; Coutinho *et al.*, 2005; Mori *et al.*, 2006). We present evidence that our model provides an excellent system to dissect the role of specific proteins in epidermal morphogenesis and wound healing events and, in so doing, may dramatically reduce the need for live animals in such research.

RESULTS

We have developed a Transwell organotypic skin model incorporating primary mouse keratinocytes and dermal fibroblasts, to probe the role of specific Cxs during epidermal morphogenesis and wound-healing events. To induce stratification and differentiation in the organotypic model, primary mouse epidermal keratinocytes were grown to confluence on Transwell polyester membranes, in the presence (Figure 1a) or absence of dermal fibroblasts (Figure 1b). Once raised to the ALI, small areas of stratification were observed throughout the keratinocyte cultures by day 1 (ALI-1) that increased in size over the following 7 days (ALI-7) to produce complex multilayered regions as determined by large flattened differentiating cells (Figure 1c). Cultures maintained in the presence of dermal fibroblasts displayed increased cellularity and the appearance of a cornified layer (Figure 1a, day 4), in comparison with cultures grown in the absence of dermal fibroblasts, where the cornified layer was less evident and delayed until day 7 (Figure 1b, day 7), thereby confirming reports by Rosdy and Clauss (1990) that keratinocytes efficiently differentiate in the absence of a fibroblast layer.

To confirm these morphological observations, dual-label immunofluorescence was performed for a number of proliferation and differentiation markers. The proliferation marker Ki67, identified by discrete nucleolar staining, was only expressed by keratinocytes in the monolayer (Figure 2a) or in the basal layer of organotypic cultures, in accordance with that observed *in vivo*. Moreover, the differentiation marker cytokeratin 10, typically expressed by suprabasal

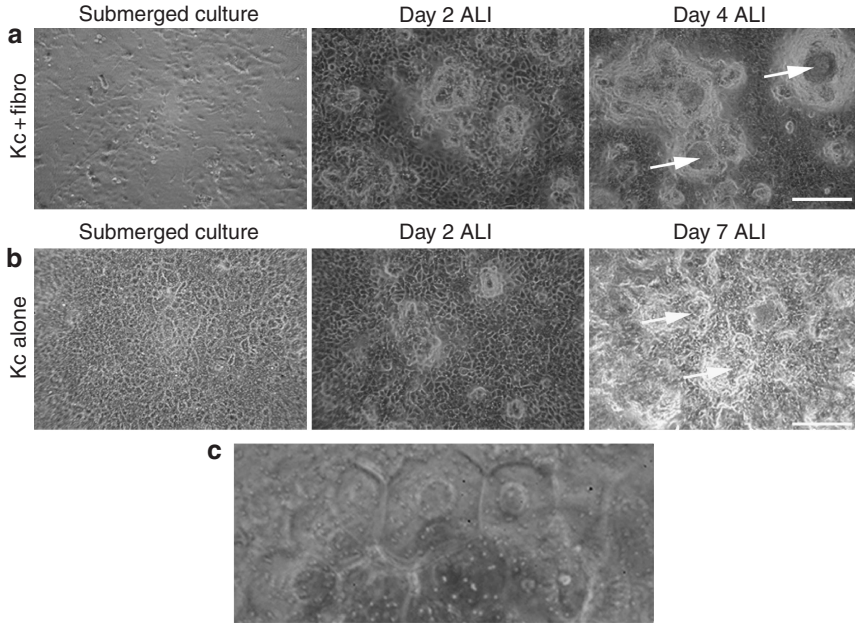

Figure 1. A complex 3D organotypic epidermis is formed when Transwell primary mouse keratinocyte monolayers are raised to the ALI in the presence or absence of dermal fibroblasts. When raised to the ALI, in the presence of dermal fibroblasts (**a**, Kc + fibro), primary mouse keratinocytes begin to stratify and terminally differentiate over a period of seven days, showing evidence of a cornified layer (arrows). Similarly, when raised to the ALI in the absence of dermal fibroblasts (**b**, Kc alone), primary mouse keratinocytes were induced to stratify and differentiate into a complex 3D tissue architecture with large flattened cells in the upper layers (**c**). Morphological differences between the two types of organotypic cultures are evident by day 4-ALI, where cultures with fibroblasts display evidence of a cornified layer, but in those without fibroblasts, a cornified layer is not evident until day 7-ALI. Bar = 100 μm.

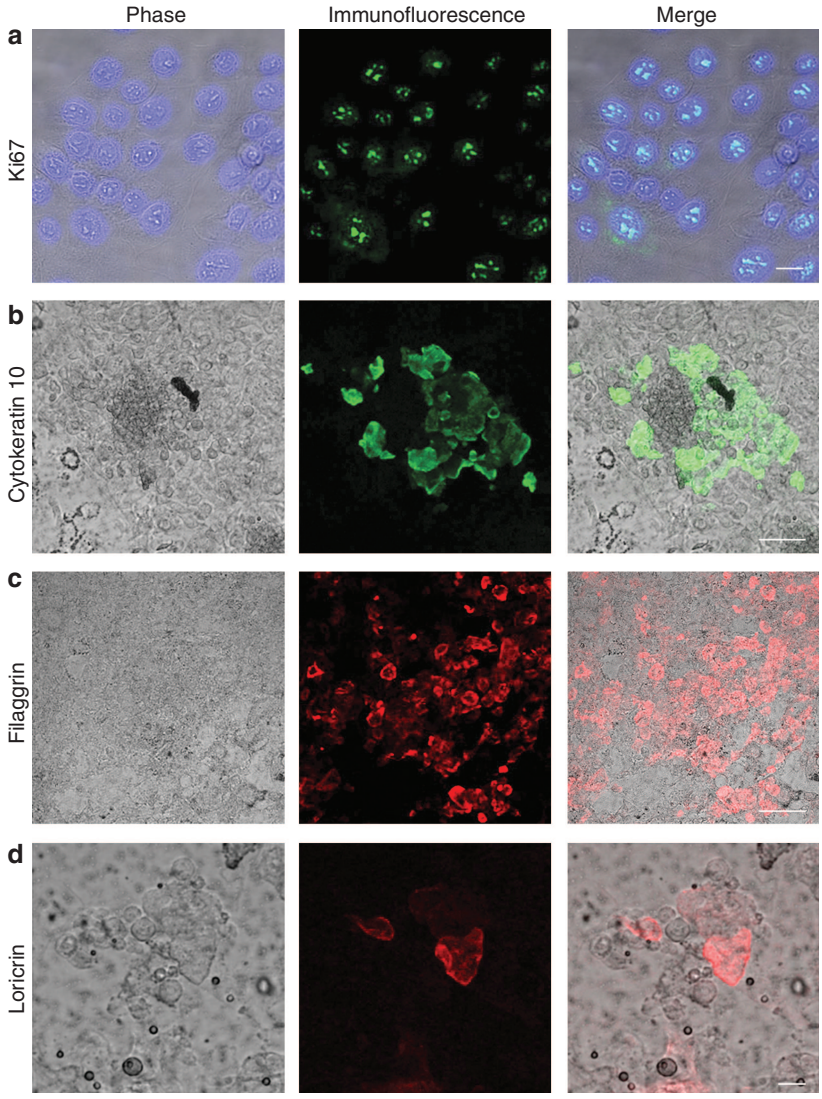

Figure 2. Transwell organotypic murine epidermis display a differentiation profile typical of that found in mouse epidermis *in vivo*. Immunofluorescence results of day 7-ALI cultures revealed that Transwell organotypic epidermis expressed several differentiation markers typically found *in vivo* in mouse epidermis. (**a**) Basal, undifferentiated keratinocytes expressed the proliferation marker, Ki67 (**a**, phase plus 4,6-diamidino-2-phenylindole (DAPI) staining illustrating cell nuclei; in the immunofluorescence image Ki67 is green and in the merged image Ki67 staining is turquoise, counterstained with DAPI blue). (**b**) In the upper, differentiating layers, cytokeratin 10 (green), a differentiation marker of suprabasal epidermal keratinocytes, was expressed, and (**c**) filaggrin expression (red), a granular layer protein, was also evident in the upper terminally differentiating layers of organotypic cultures. (**d**) In the uppermost keratinocyte layers, the cornified envelope protein, loricrin (red), was also expressed. (**a** and **d**) Bar = 10 μm; (**b** and **c**) bar = 100 μm.

keratinocytes, was located in the stratifying and differentiating regions of the organotypic models (Figure 2b). Presence of the granular layer was confirmed by staining for filaggrin (Figure 2c) and finally, loricrin, a cornified envelope protein, confirmed terminal differentiation of the uppermost cells within the skin model even in the absence of fibroblasts (Figure 2d). Thus, keratinocytes in our organotypic skin model efficiently differentiate, in the presence or absence of dermal fibroblasts, to form a ''living skin'' equivalent that reflects the differentiation status normally found *in vivo* within mouse epidermis (Butterweck *et al.*, 1994).

Cx26, Cx30, and Cx43 are differentially expressed in murine organotypic epidermis, with a Cx profile typical of that observed *in vivo*

Previous studies have shown that epidermal keratinocytes express a number of Cxs including Cx26, Cx30.3, Cx31, Cx31.1, Cx40, and Cx43 (Di *et al.*, 2001a). Cx43, in particular, is localised to the undifferentiated basal layer of mouse epidermis *in vivo*, with Cx26 and Cx30 confined to the upper, differentiated epidermal layers (Risek *et al.*, 1992; Kretz *et al.*, 2003; Maher *et al.*, 2005). Whole-mount dual indirect immunofluorescence and 3D Z-Stack reconstruction of organotypic epidermis were performed using Cx antibodies

targeting Cx26, Cx30, and Cx43, to determine the Cx distribution in the epidermal cultures. Extensive Cx43 expression was observed in the basal, undifferentiated keratinocytes, with limited expression in the upper, differentiating layers (Figure 3a). By contrast, the distribution pattern of Cx26 expression was restricted to the uppermost keratinocyte populations and was absent in the basal layer. Cx30 and Cx26 gap junction plaques were only noted between the flattened cells of the upper differentiated layers where they often colocalised (Figures 3b and 1c), consistent with observations in normal mouse epidermis (Goliger and Paul, 1995; Kretz *et al.*, 2003). 3D Z-stack reconstruction also revealed the differential localisation of Cx43 in the basal layer and presence of cytokeratin 10 in the suprabasal layers (Figure 3c).

Following wounding, murine organotypic epidermis retains the potential for re-epithelialisation

We aimed to exploit this model to investigate the role of specific Cxs during wound-healing events. Wound healing is a complex event, but, in the epidermis, essentially involves the coordinated migration of keratinocytes from the intact epidermis to form a monolayer over the wound bed, with subsequent stratification and terminal differentiation events. Organotypic epidermal cultures, raised to ALI-4 and showing regions of stratification and differentiation, were wounded and keratinocyte migration into the wound bed was recorded on a daily basis. During the first 3–4 days following wounding, keratinocytes migrated outward into the wound bed to form an intact monolayer between the two wound edges (Figure 4a). At this stage, following the formation of this intact keratinocyte monolayer, two distinct modes of wound closure were observed, which resulted in the regeneration of an intact organotypic epidermis. The first method of wound closure (Figure 4b) demonstrated gradual inward closure of the wound, whereby the opposing wound margins were pulled together to finally close the wound and form an intact organotypic epidermis. The second mode (Figure 4c) involved the stratification of distinct regions of cells within the center of a keratinocyte monolayer. Over time, these stratifying regions increased in size, spreading outward toward each wound edge, terminally differentiating, and eventually joining with the existing wounded epidermal edges. The results reveal that our organotypic epidermal skin model retains the ability to regenerate following wounding, and permits detailed observation of the process of closure and restratification.

Primary mouse keratinocytes demonstrate extensive gap junction intercellular communication (GJIC) properties

The proliferative monolayer displayed numerous Cx43 gap junction plaques between adjoining cells (Figure 5a); however, Cx26 and Cx30 gap junction plaques were not detected in these undifferentiated keratinocyte populations (data not shown). In order to determine whether the Cx43 gap junction channels observed between keratinocytes were functional, confluent monolayers were microinjected with a variety of gap junction-permeable tracers including neurobiotin, AlexaFluor 488 (data not shown), and AlexaFluor 594 that are efficiently transferred by Cx43 channels, but have limited permeation through Cx26 and presumably Cx30 channels (JA Easton and PE Martin, unpublished observations; Nicholson *et al.*, 2000). Following injection of all tracers, dye spread to several adjacent keratinocytes was observed, demonstrating functional gap junctional coupling (Figure 5b). Organotypic cultures were similarly able to form functional gap junction channels (not shown).

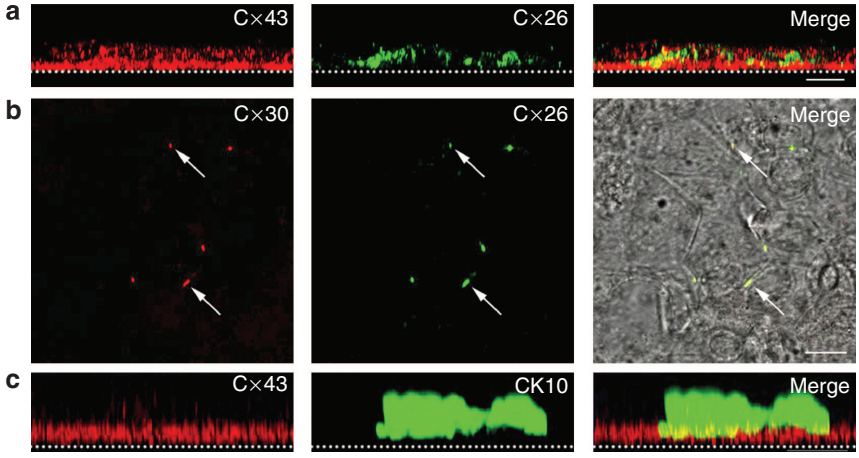

Figure 3. The Cx expression profile of murine organotypic cultures is comparable to that observed in mouse epidermis *in vivo*. (**a**) 3D Z-Stack reconstruction following dual-label immunofluorescence targeting Cx26 and Cx43 expression in day 7-ALI cultures revealed Cx43 (red) and Cx26 (green) to be differentially and spatially expressed within organotypic epidermis. Cx43 staining was displayed by basal and suprabasal keratinocytes, whereas Cx26 expression was confined to the upper more differentiated keratinocytes, with little overlap of either distribution pattern (merge). (**b**) In the upper layers, Cx30 (red, arrow) and Cx26 (green, arrow) expression was detected at intercellular junctions between differentiated keratinocytes often demonstrating colocalisation (merge, arrow). (**c**) 3D Z-Stack reconstruction of Cx43 and cytokeratin 10 immunofluorescence in organotypic cultures demonstrated correct spatial Cx43 (red) expression within the basal layer and cytokeratin 10 staining (green) of suprabasal keratinocytes. Dotted line indicates the edge of the Transwell membrane. (**a** and **c**) Bar = 100 μm; (**b**) bar = 20 μm.

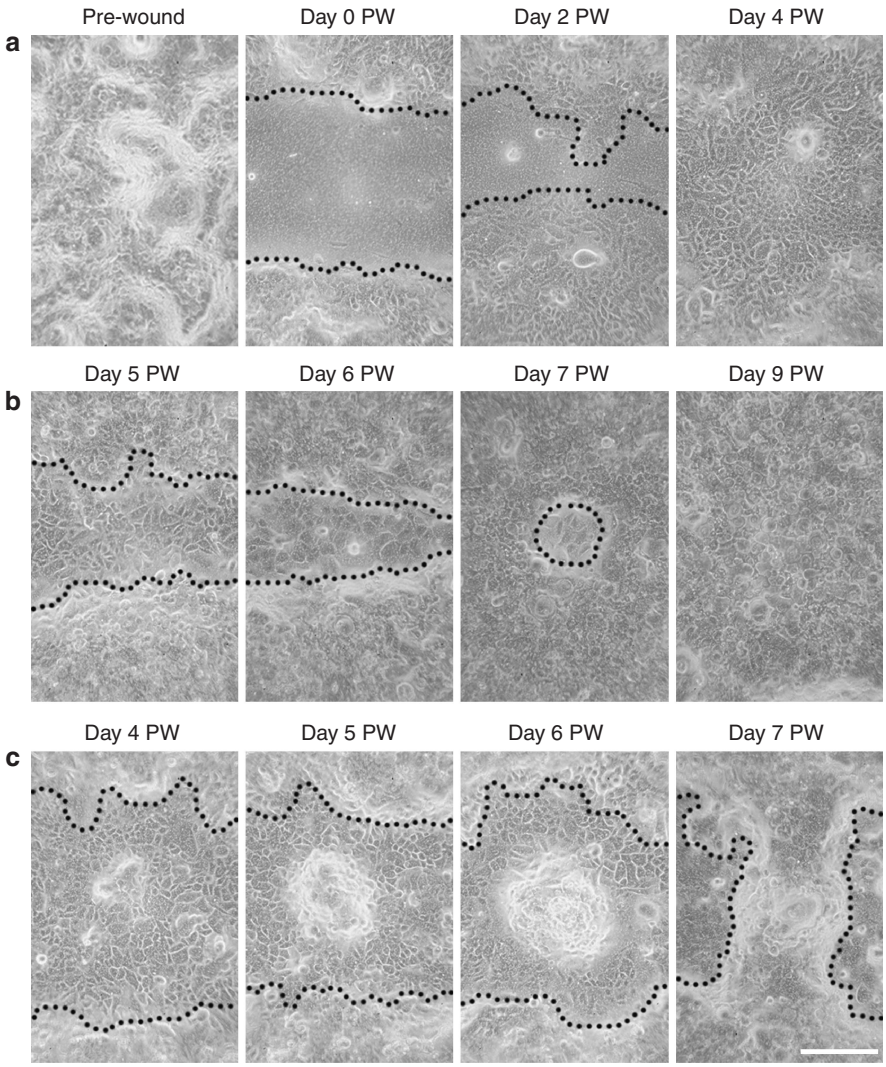

Figure 4. Wounding of raised cultures initiates mouse keratinocyte migration out of a stratified organotypic epidermis to form an intact monolayer that covers the wound bed. (**a**) Using a simple scratch assay, organotypic epidermal cultures (ALI-4) were wounded by introducing a linear cut through the cells using a sterile 10-μl pipette tip, and keratinocyte migration was monitored daily. Over the following 3 days post-wounding, keratinocyte migration was observed from both wound margins toward the center of the wound, with an intact keratinocyte monolayer formed by day 4 post-wounding. Two modes of wound closure and re-epithelialisation were observed in wounded organotypic cultures. (**b**) The first mode displayed gradual epidermal closure toward the center of the wound over a period of 4 days. (**c**) The second mode of wound closure demonstrated increasing keratinocyte stratification within the center of the wound bed, with terminal differentiation to form epidermal bridges between opposing wound margins, with complete wound closure observed over a period of 4 days. Dotted lines indicate boundary areas of stratified and non-stratified areas. Bar = 50 μm.

Wound closure is accelerated in murine epidermal organotypic cultures treated with the Cx mimetic peptide Gap27

Cx expression is known to be altered during wound healing, in particular, Cx43 expression is reduced at the wound edge, and there is evidence that specific knockdown of Cx43 can enhance keratinocyte migration and wound-healing responses (Qiu *et al.*, 2003; Mori *et al.*, 2006). Cx mimetic peptides acutely inhibit Cx-mediated communication by inhibiting gap junction channel formation, rather than knocking down Cx expression in cells (Evans and Boitano, 2001; Martin *et al.*, 2005). Microinjection of keratinocytes with AlexaFluor 594 showed that GJIC was significantly reduced following treatment of the cells with Cx mimetic peptides Gap27, ($P<0.05$) (Figure 5d) and Gap26M (not shown). Immunolocalisation analysis illustrated that the peptides did not alter Cx43 distribution in gap junction plaques at points of cell-to-cell contact in the plasma membrane (Figure 5c). Collectively, these results support the concept that the Cx mimetic peptide, Gap27, acts by inhibiting Cx43 channel functionality, rather than altering Cx43 expression levels.

To determine whether Gap27 treatment had any effect upon cell migration following wounding, a scratch wound assay was performed in mature organotypic cultures. In control samples (Figure 6a), keratinocytes at the wound margin began to slowly migrate outwards after day 1 post-wounding and final wound closure was observed four days post-wounding. Accelerated keratinocyte migration was

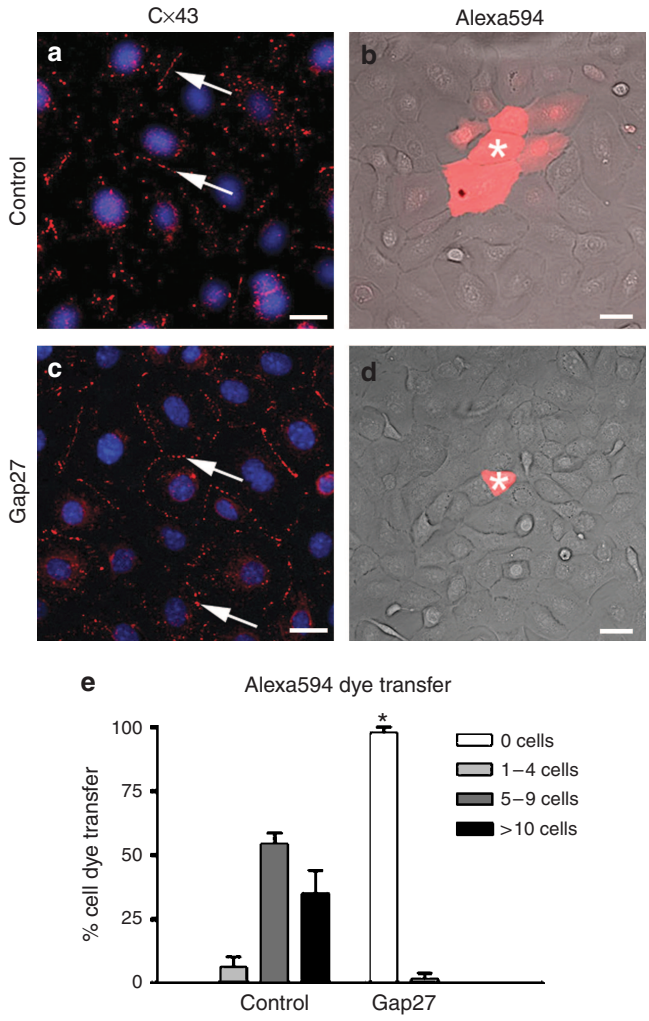

Figure 5. Primary mouse keratinocytes are coupled predominantly by Cx43-based gap junction channels and, following treatment with the Cx mimetic peptide, Gap27, display reduced GJIC. Cx43 gap junction plaques were detected by indirect immunofluorescence in untreated mouse keratinocyte monocultures (**a**, red with DAPI nuclei counterstain, blue) that demonstrated efficient transfer of the Cx43-permeable Alexa 594 dye (**b**). (**c**) Treatment with the Cx mimetic peptide, Gap27 (100 μM), did not alter Cx43 distribution patterns in treated cells as Cx43 gap junction plaques were still observed at the plasma membrane in comparable levels to untreated cells (**a**). However, Gap27 treatment (100 μM) significantly inhibited Alexa 594 dye transfer in primary mouse keratinocytes (**d**) in comparison to untreated cells (**b**). Gap27 dye transfer studies are summarised in (**e**) and demonstrate a significant reduction in GJIC properties of Gap27-treated keratinocytes. Microinjected cells are indicated with an asterisk; $n = 3$, with approximately 30 cells per experiment; $P < 0.05$. Bar = 20 μm. Arrows indicate GJ plaques.

observed in mouse keratinocytes treated with Gap27 (Figure 6a), where wound closure was observed at day 2 post-wounding (Figure 6a), when cells had migrated into the wound space and completely filled the wound. The results indicated that following Gap27 treatment, 50% wound closure was achieved by 24 hours; by contrast, in untreated cells 50% wound closure took up to 52 hours (Figure 6b). Following wound closure both peptide-treated and control cells took 7–8 days to form a stratified and differentiated organotypic epidermis (Figure 6c). The Cx mimetic peptides also enhanced the migration rates of human dermal fibroblasts and keratinocytes into a ''wound bed''. By contrast a scrambled peptide had no effect on cell migration rates compared with control cells where no peptide was added, thereby confirming the specificity of Gap27 in modifying these events (CS Wright and PE Martin, unpublished observations).

DISCUSSION

We report the development of a Transwell organotypic murine skin model derived from primary mouse keratinocytes, which has enabled, in a complex 3D environment, investigation into the important cellular events that occur during epidermal morphogenesis and wound re-epithelialisation. This reconstructed organotypic system displays morphological and differentiation characteristics typical of those observed *in vivo* and possesses a number of practical advantages over human-based and the even fewer murine organotypic models that are currently available. The majority of organotypic epidermal models are unable to provide the vital *in situ* visualisation of cell–cell interactions and organisation within a complex 3D setting as most are dependent upon histological processing (Carroll and Moles, 2000; El-Ghalbzouri *et al.*, 2002; Ikuta *et al.*, 2006). Employing semipermeable Transwell culture chambers that are transparent under phase-contrast microscopy and exhibit no autofluorescence our model has overcome this challenge. The optical transparency provides a unique and non-invasive *in vitro* system, ideally suited to real-time analysis and a variety of integrated *in situ* imaging techniques, which negates the need for arduous histological processing. Additionally, the porous nature of the Transwell inserts enables diffusion of soluble nutrients and factors from the culture medium and may also enhance cell attachment rates (McMillan *et al.*, 2007).

The model was validated on the basis of tissue morphology and architecture, in conjunction with the expression of keratinocyte differentiation markers and cornified envelope proteins. The differentiation status of the organotypic cultures was readily determined by exploiting the unique imaging properties of the model and verified that by phase-contrast microscopy and whole-mount immunofluorescence, the *in vitro* system expressed the differentiation markers characteristic of murine epidermis. The proliferation marker Ki67 was expressed in the basal layer of organotypic epidermis, whereas the upper suprabasal layers displayed cytokeratin 10 and filaggrin staining, with loricrin expression restricted to the uppermost terminally differentiated cells of the cornified layer. These results indicated a mature organotypic system, with features comparable to those *in vivo*, which could potentially provide the opportunity to examine important aspects of integrated cellular behavior during wound healing and epidermal re-epithelialisation.

To evaluate this possibility, a wound was introduced to mature organotypic cultures with a complex 3D tissue architecture. Primary mouse keratinocytes migrated out from

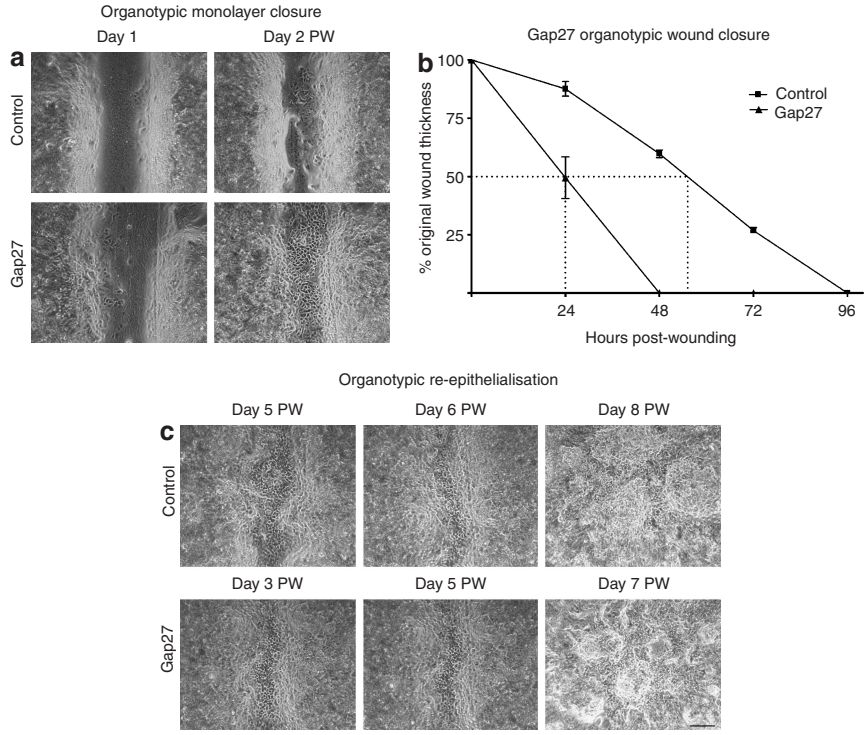

Figure 6. Following treatment with the Cx mimetic peptide, Gap27, wound closure is enhanced in wounded organotypic epidermis. (**a**) Following a simple wound assay, cells treated with Gap 27 migrated into and filled the ''gap'' within 2 days compared with control cells where closure took up to 4 days. q(**b**) Quantification of wound healing rates shows that 50% wound closure was achieved by 24 hours in Gap27-treated cultures compared with control cultures that took up to 52 hours. (**c**) Subsequent re-epithelialisation under both conditions took up to 8 days; $n = 3$.

a fully stratified organotypic epidermis to form an intact monolayer covering the wound bed, with subsequent stratification and differentiation of keratinocytes, to reform intact epidermal layers. Significantly, this study is the first to demonstrate real-time visualisation of cellular events occurring during the regeneration of murine organotypic epidermis, and revealed two distinct methods of wound re-epithelialisation within the 3D cultures.

The first observed mode of wound closure displayed characteristic migration of basal keratinocytes out from the wound margins to produce an intact monolayer of cells covering the wound site. The organotypic epidermal margins gradually moved inwards to close the wound and restore epidermal integrity. Previous wounding studies acknowledge a wound closure pattern that resembles this mode of wound closure (Usui *et al.*, 2005). The second observed mode of wound closure, to our knowledge, has not been reported. In this instance, following keratinocyte monolayer production, keratinocyte stratification occurred in the center of the wound bed and subsequent differentiation resulted in the formation of epidermal ''bridges'' that linked the wound margins. The epidermal ''bridges'' continued to develop and grow in size to create a fully stratified and terminally differentiated epidermis. This mode of wound closure has similarities to the ''purse and string'' system reported during embryonic wound-healing events (Martin and Lewis, 1992; Brock *et al.*, 1996).

The versatility of the model enabled us to functionally probe, image, and analyze the coordination of cellular activities via the integrated gap junction network that exists within the skin. Keratinocytes spatially express Cxs in specific and often overlapping patterns within the differentiating layers of the epidermis (Salomon *et al.*, 1994). Reverse transcription-PCR analysis (data not shown) revealed that the Cx expression profile of primary mouse keratinocytes included all the epidermal Cxs reported from previous literature (Cx26, Cx30, Cx31, Cx43) and also those not (Cx37, Cx40, Cx45) previously reported (Kamibayashi *et al.*, 1993; Butterweck *et al.*, 1994; Goliger and Paul, 1995; Choudhry *et al.*, 1997; Kretz *et al.*, 2003). A major advantage of our model is its ability to evaluate the tissue architecture and spatial localisation of a varied spectrum of epidermal proteins by whole-mount immunolocalisation. In this study we used high-resolution laser scanning confocal microscopy followed by 3D Z-Stack reconstruction to illustrate that the model reflected the Cx expression profile of intact mouse epidermis, with Cx26, Cx30, and Cx43 being differentially expressed. In the organotypic model Cx43 was localised to the basal and lower suprabasal layers, whereas Cx26 and Cx30 were restricted to the upper differentiated layers of organotypic epidermis, confirming the correct Cx expression repertoire observed in murine epidermis *in vivo* (Kamibayashi *et al.*, 1993; Butterweck *et al.*, 1994).

Remodelling of this versatile Cx network within the epidermis is associated with a variety of pathophysiological conditions including psoriasis and the ability of wounds to heal (Goliger and Paul, 1995; Labarthe *et al.*, 1998; Lucke *et al.*, 1999; Kretz *et al.*, 2003). Mutations in Cxs are also

associated with a host of genetically inherited skin disorders for which a variety of transgenic mice models are now available (see reviews by White and Paul, 1999; Willecke *et al.*, 2002). The molecular mechanisms underlying these events and the role of specific Cxs in cell migration and proliferation responses remain unresolved. The organotypic model system so developed permits us to begin to employ a spectrum of Cx-specific knockdown technologies, including the use of Cx-specific mimetic peptides and short interfering RNA (siRNA) resources combined with Cx knockout and transgenics *in vivo* models, to determine the mechanistics of Cx-mediated communication within the skin during epidermal development and pathophysiological events. Specific post-transcriptional gene silencing by siRNA has facilitated the study of single gene knockdown in conventional cultures of mammalian cells (Elbashir *et al.*, 2001; Harborth *et al.*, 2001; Bantounas *et al.*, 2004) and, more recently, in a complex 3D *in vitro* system (Mildner *et al.*, 2006). The latter study demonstrated efficient gene silencing in an organotypic skin model that examined targeted gene silencing in epidermal development and differentiation. Potentially, siRNA resources could provide an alternative approach to gene deletion animal models, which can give rise to a lethal phenotype and open up avenues for a reduction in animal experimentation. The recent finding that siRNA was transferable by mammalian cells expressing Cx43, but not Cx26 or Cx30, channels (Valiunas *et al.*, 2005) indicates that siRNA technologies present an attractive strategy to enable targeted gene deletion in a complex 3D setting that could probe the roles of specific Cxs during epidermal events. Cx43 expression is greatly reduced following wounding, and in keratinocytes, migration across the wound bed, suggesting that altered Cx43 expression may be an important feature facilitating wound closure (Coutinho *et al.*, 2003, 2005; Qiu *et al.*, 2003; Brandner *et al.*, 2004). Indeed, topical application of antisense Cx43 oligodeoxyribonucleotides enhanced wound closure in a mouse wounding model (Qiu *et al.*, 2003), and rates of wound healing were modified in Cx-deficient mice (Kretz *et al.*, 2003), thus emphasising the important role of Cxs in cell proliferation and migration events. These approaches result in the knockdown of Cx expression and function, and so the exact role of Cx-mediated communication *versus* Cx expression is not fully dissected, with controversy over the role of Cx ''channel activity'' and non-channel active roles in the control of cell growth responses (Kardami *et al.*, 2007).

In this study we investigated the effect of acute inhibition of GJIC with small Cx-specific mimetic peptides on cell migratory responses following wounding in our 3D organotypic model system. These peptides are targeted to the extracellular loops of Cxs and have been widely employed to determine the role of specific Cxs in diverse tissue systems including the vasculature (Isakson and Duling, 2005; Martin *et al.*, 2005) and immune system (see review by Evans and Boitano, 2001). In our model system Cx mimetic peptides significantly decreased levels of cell-to-cell communication through Cx43 gap junction channels, but did not alter the presence of gap junction plaques at the cell membrane, thereby supporting previous findings in vascular cells (Martin *et al.*, 2005). In this study, wounded primary mouse keratinocyte monolayers or 3D organotypic cultures treated with the Cx mimetic peptide, Gap27, displayed enhanced migration and wound closure rates twice those of untreated cells, illustrating for the first time that acute inhibition of GJIC by Cx mimetic peptides can modify cell growth responses. These observations support data from *in vivo* wound healing studies where antisense oligonucleotides targeted to Cx43 increased wound closure rates by enhancing keratinocyte migration and fibroblast migration rates (Mori *et al.*, 2006). Thus, Cxs are emerging as attractive therapeutic targets, particularly as it is now evident that chronic conditions such as non-healing diabetic wounds have increased Cx expression associated with the wound edge and tools such as Cx mimetic peptides permit probing of the down stream consequences of acutely blocking Cx function without altering the protein expression level. Such downstream events may involve the ability of cells within a wound to coordinate cellular activities associated with cell migratory and inflammatory responses (Mori *et al.*, 2006; Neub *et al.*, 2007).

In vivo wound healing studies are invasive by nature, with varying degrees of severity that can cause considerable stress and discomfort to the animals involved. Therefore, there is a growing need for the development of a rapid and reliable 3D organotypic skin model that can reproducibly exhibit *in vivo*-like morphological and growth characteristics. Significantly, the *in vitro* system detailed in this study opens up avenues for the potential reduction of animal experimentation/manipulation, as a single litter of perinatal mice can generate sufficient material for extensive experiments. This model offers an attractive and versatile imaging tool to evaluate the effect of potential therapeutic targets on the rate of wound re-epithelialisation in real time, and functionally probe the role specific Cxs play during epidermal development and organisation.

MATERIALS AND METHODS

Primary mouse keratinocyte isolation

Mice were maintained in accordance with local governmental and institutional animal care regulations, and all procedures had institutional approval. The skin was removed from sacrificed perinatal pups less than 2 days old, and processed with minor modifications as described by Mazzalupo *et al.* (2002). The resulting epidermal cell suspension was pelleted and resuspended in progenitor cell targeted epidermal keratinocyte medium (Chemicon, Cambridge, UK) and calcium-free DMEM (Invitrogen, Paisley, UK) containing 10% chelexed fetal bovine serum. Cells were seeded at a density of 1×10^6 cells/ml in appropriate culture vessels, and left to adhere overnight in a humidified atmosphere at 37°C with 5% CO_2.

Dermal fibroblast explant culture

Following epidermal–dermal separation, the dermal tissue was washed in fetal bovine serum for 5 minutes to inactivate trypsin activity and, using a sterile scalpel blade, finely chopped and placed in 1 ml DMEM (Invitrogen) containing 10% fetal bovine serum. This suspension was placed in sterile culture flasks and left to adhere overnight before adding fresh DMEM plus 10% fetal bovine serum.

After approximately 4–5 days, confluent fibroblasts were passaged in 0.25% trypsin solution, seeded onto the underside of the Transwell insert membranes, and left to adhere overnight; the following day, fresh medium was added to the lower Transwell chamber.

Preparation and maintenance of organotypic cultures

In order to grow organotypic epidermis, a 1×10^6-cells/ml suspension of freshly harvested keratinocytes was seeded directly onto Transwell polyester culture inserts (12 or 24 mm; Sigma, Poole, Dorset, UK), in the presence or absence of dermal fibroblasts on the underside. Keratinocyte growth medium was placed in both the upper and lower chambers and cells were left to adhere overnight in a humidified atmosphere at 37°C with 5% CO_2. The cells were washed daily in calcium-free phosphate-buffered saline (Cambrex, Wokingham, UK) and keratinocyte growth medium was replaced until a confluent monolayer of cells was obtained. At confluence, the keratinocyte growth medium was removed from the upper chambers to expose the cells to the ALI, and cells were cultured for up to 2 weeks with daily lower chamber medium changes.

Immunofluorescence

Dual and triple immunofluorescent labelling with Cx, proliferation, and differentiation markers by standard and whole-mount laser scanning confocal microscopy was used to characterise both the monolayer and organotypic epidermal cultures. Briefly, monolayers plated on glass chamber slides (1×10^6 cells/ml) and organotypic cultures were fixed in ice-cold methanol for 10 minutes and processed as described by Martin *et al.* (2005). Cx expression was analyzed using rabbit anti-Cx43 (1:1000; kindly gifted by Dr Edgar Rivedal, Norway), mouse anti-Cx26 (1:200; 13-8100, Zymed Laboratories Inc., San Francisco, CA), and rabbit anti-Cx30 (1:100; 71-6100, Zymed Laboratories Inc). A monoclonal antibody targeted to β-tubulin was also used (1:100, T4026; Sigma). To assess the degree of differentiation in the organotypic epidermis, mouse anti-keratin 10 (1:50, ab9025; Abcam, Cambridge, UK), rabbit anti-filaggrin (1:50; kindly gifted by Professor Irwin McClean), and rabbit anti-loricrin (1:50, ab24722; Abcam) antibodies were used. In addition, the proliferation status of cells was examined by employing a goat anti-Ki67 antibody (1:50, sc-7846; Santa Cruz, CA, via Autogen Bioclear, Calne, UK). Secondary anti-mouse, -rabbit, and -goat antibodies conjugated to either AlexaFluor 488 or AlexaFluor 594 (1:500; Molecular Probes, Eugene, OR, via Invitrogen) were used. Finally, cell nuclei were counterstained with DAPI (10 ng/ml, w/v in phosphate-buffered saline). Immunolabelled cultures were viewed under a ×40 oil-immersion lens mounted on a Zeiss 200 Axioscope microscope linked up to a Zeiss LSM 510 META laser scanning system, using the following settings: Alexa 488 was excited using the Argon laser at 488 nm excitation and emission at 500–550 nm. Alexa 594 was excited with a Helium Neon laser at 543 nm excitation and emission at 600–650 nm. Images were further processed using Adobe Photoshop software.

Microinjection

To assess the gap junctional dye transfer properties of mouse keratinocytes in monolayer in the presence or absence of the Cx mimetic peptide, Gap27, cells were pressure-microinjected with 10 mM AlexaFluor594 (molecular weight 759 Da; Molecular Probes, via Invitrogen) using an Eppendorf 5120 FemtoJet system linked up to a Nikon 200 inverted microscope. Cells were fixed in 3.7% formaldehyde for 5 minutes and dye spread to neighboring cells was recorded for each microinjected cell. The effect of the Gap27 was quantified by determining the percentage of cells showing dye transfer comparable to untreated cells with >30 keratinocytes assessed per experiment, and each experiment repeated in triplicate. Images were recorded using a Zeiss LSM 510 Meta system and analyzed with Adobe Photoshop software.

Effect of Gap27 mimetic peptide on wound closure

Gap27, a peptide with sequence homology to the ''gap'' sequence of the second extracellular loop of Cx43 (^{43}Gap27), ''SRPTEKTIFFI'' (Evans and Boitano, 2001; Martin *et al.*, 2005), was used to assess whether the rate of keratinocyte wound closure could be altered following knockdown of Cx functionality. The peptide (w/v, 100 μM in serum-free keratinocyte growth medium) was applied daily to confluent keratinocyte monolayers or wounded organotypic cultures.

Wound assay

To assess keratinocyte migration following wounding of organotypic epidermis, in the presence or absence of Cx mimetic peptide, scratch assays were performed. A sterile 10-μl pipette tip was used to create a wound in either confluent keratinocyte monolayers or organotypic cultures raised to ALI-4 with daily medium changes thereafter.

Using a Nikon Eclipse TS100 inverted microscope and CMEX-1300 digital camera, organotypic wounds were observed and recorded on a daily basis until re-epithelialisation was achieved. Keratinocyte migration was measured using Euromex ImageFocus analyzing software, and images were then processed with Adobe Photoshop software. Briefly, 10 measurements were taken within three separate fields of view of a single wounded culture. As far as possible and using the same method, the same regions were then measured and recorded on a daily basis. Experiments were repeated in triplicate using different litters of mice and measurements were reported as an average of percentage wound closure against the initial wound distance taken immediately after insult. Fifty percent wound closure rates were then determined following data analysis, using Prism software.

Statistical analysis

Data were analyzed by Student's *t*-test, with $P<0.05$ being considered significant.

CONFLICT OF INTEREST

The authors state no conflict of interest.

ACKNOWLEDGMENTS

We would like to acknowledge Veronica Graham and Brian Leiper for their support and assistance in obtaining animal tissue for our studies. We would also like to thank Dr Edgar Rivedal for kindly providing the Cx43 polyclonal antibody, Professor Irwin McLean for gifting the filaggrin polyclonal antibody used in this study, and Zealand Pharma for supply of Cx mimetic peptides. This work was supported by the Biotechnology and Biological Sciences Research Council (BBSRC) Grant no. BB/C005058.

REFERENCES

Arita K, Akiyama M, Tsuji Y, McMillan JR, Eady RAJ, Shimizu H (2002) Changes in gap junction distribution and connexin expression pattern during human fetal skin development. *J Histochem Cytochem* 50:1493–500

Bakirtis G, Choudhry R, Aasen T, Shore L, Brown K, Bryson S *et al.* (2003) Targeted epidermal expression of mutant connexin 26 (D66H) mimics true Vohwinkel syndrome and provides a model for the pathogenesis of dominant connexin disorders. *Hum Mol Genet* 12:1737–44

Bantounas I, Phylactou LA, Uney JB (2004) RNA interference and the use of small interfering RNA to study gene function in mammalian systems. *J Mol Endocrinol* 33:545–57

Brandner JM, Houdek P, Husing B, Kaiser C, Moll I (2004) Connexins 26, 30, and 43: differences among spontaneous, chronic and accelerated human wound healing. *J Invest Dermatol* 122: 1310–1320

Brock J, Midwinter K, Lewis J, Martin P (1996) Healing of incisional wounds in the embryonic chick wing bud: characterization of the actin purse-string and demonstration of a requirement for Rho activation. *J Cell Biol* 135:1097–107

Butterweck A, Gergs U, Elfgang C, Willecke K, Traub O (1994) Differential expression of the gap junction proteins connexin45, 43, 40, 31, and 26 in mouse skin. *Eur J Cell Biol* 65:152–63

Carroll JM, Moles JP (2000) A three-dimensional skin culture model for mouse keratinocytes: application to transgenic mouse keratinocytes. *Exp Dermatol* 9:20–4

Choudhry R, Pitts JD, Hodgins MB (1997) Changing patterns of gap junctional communication and connexin distribution in mouse epidermis and hair follicles during embryonic development. *Dev Dyn* 210:417–30

Common JE, Becker D, Di WL, Leigh IM, O'Toole EA, Kelsell DP (2002) Functional studies of human skin disease- and deafness-associated connexin 30 mutations. *Biochem Biophys Res Commun* 298:651–6

Coutinho P, Qui C, Frank S, Tamber K, Becker D (2003) Dynamic changes in connexin expression correlate with key events in the wound healing process. *Cell Biol Int* 27:525–41

Coutinho P, Qui C, Frank S, Wang CM, Brown T, Green CR *et al.* (2005) Limiting burn extension by transient inhibition of connexin43 expression at the site of injury. *Br J Plast Surg* 58:658–67

Di WL, Common JE, Kelsell DP (2001b) Connexin 26 expression and mutation analysis in epidermal disease. *Cell Commun Adhes* 8:415–58

Di WL, Rugg EL, Leigh IM, Kelsell DP (2001a) Multiple epidermal connexins are expressed in different keratinocyte subpopulations including connexin 31. *J Invest Dermatol* 117:958–64

Elbashir SM, Harborth J, Lendeckel W, Yalcin A, Weber K, Tuschl T (2001) Duplexes of 21-nucleotide RNAs mediate RNA interference in cultured mammalian cells. *Nature* 411:488–94

El-Ghalbzouri A, Gibbs S, Lamme E, Van Blitterswijk CA, Ponec M (2002) Effect of fibroblasts on epidermal regeneration. *Br J Dermatol* 147: 230–43

Essenfelder GM, Bruzzone R, Lamartine J, Charollais A, Blanchet-Bardon C, Barbe MT *et al.* (2004) Connexin30 mutations responsible for hidrotic ectodermal dysplasia cause abnormal hemichannel activity. *Hum Mol Genet* 13:1703–14

Evans WH, Martin PE (2002) Gap junctions: structure and function (review). *Mol Membr Biol* 19:121–36

Evans WH, Boitano S (2001) Connexin mimetic peptides: specific inhibitors of gap-junctional intercellular communication (review). *Biochem Soc Trans* 29:606–12

Goliger JA, Paul DL (1995) Wounding alters epidermal connexin expression and gap junction-mediated intercellular communication. *Mol Biol Cell* 6:1491–501

Harborth J, Elbashir SM, Bechert K, Tuschl T, Weber K (2001) Identification of essential genes in cultured mammalian cells using small interfering RNAs. *J Cell Sci* 114:4557–65

Harrison CA, Heaton MJ, Layton CM, MacNeil S (2006) Use of an *in vitro* model of tissue-engineered human skin to study keratinocyte attachment and migration in the process of re-epithelialization. *Wound Repair Regen* 14:203–9

Ikuta S, Sekino N, Hara T, Saito Y, Chida K (2006) Mouse epidermal keratinocyte in three-dimensional organotypic coculture with dermal fibroblasts form a stratified sheet resembling skin. *Biosci Biotechnol Biochem* 70:2669–75

Isakson BE, Duling BR (2005) Heterocellular contact at the myoendothelial junction influences gap junction organization. *Circ Res* 97: 44–51

Kamibayashi Y, Oyamada M, Oyamada Y, Mori M (1993) Expression of gap junction proteins connexin 26 and 43 is modulated during differentiation of keratinocytes in newborn mouse epidermis. *J Invest Dermatol* 101:773–8

Kardami E, Dang X, Iacobas DA, Nickel BE, Jeyaraman M, Srisakuldee W *et al.* (2007) The role of connexins in controlling cell growth and gene expression. *Prog Biophys Mol Biol* 94:245–64

Kelly SC, Ratajczak P, Keller M, Purcell SM, Griffin T, Richard G (2006) A novel GJA 1 mutation in oculo-dento-digital dysplasia with curly hair and hyperkeratosis. *Eur J Dermatol* 16:241–5

Kretz M, Euwens C, Hombach S, Eckardt D, Teubner B, Traub O *et al.* (2003) Altered connexin expression and wound healing in the epidermis of connexin-deficient mice. *J Cell Sci* 116:3443–52

Labarthe MP, Bosco D, Saurat JH, Meda P, Salomon D (1998) Upregulation of connexin 26 between keratinocytes of psoriatic lesions. *J Invest Dermatol* 111:72–6

Laird DW (2006) Life cycle of connexins in health and disease. *Biochem J* 394:527–43

Lucke T, Choudhry R, Thom R, Selmer IS, Burden AD, Hodgins MB (1999) Upregulation of connexin26 is a feature of keratinocyte differentiation in hyperproliferative epidermis, vaginal epithelium, and buccal epithelium. *J Invest Dermatol* 112:354–61

Macari F, Landau M, Cousin P, Mevorah B, Brenner S, Panizzon R *et al.* (2000) Mutation in the gene for connexin 30.3 in a family with erythrokeratodermia variabilis. *Am J Hum Genet* 67:1296–301

Maestrini E, Korge BP, Ocana-Sierra J, Calzolari E, Cambiaghi S, Scudder PM *et al.* (1999) A missense mutation in connexin26, D66H, causes mutilating keratoderma with sensorineural deafness (Vohwinkel's syndrome) in three unrelated families. *Hum Mol Genet* 8:1237–43

Maher AC, Thomas T, Riley JL, Veitch G, Shao Q, Laird DW (2005) Rat epidermal keratinocytes as an organotypic model for examining the role of Cx43 and Cx26 in skin differentiation. *Cell Commun Adhes* 12:219–30

Martin P, Lewis J (1992) Actin cables and epidermal movement in embryonic wound healing. *Nature* 360:179–83

Martin PE, Wall C, Griffith TM (2005) Effects of connexin-mimetic peptides on gap junction functionality and connexin expression in cultured vascular cells. *Br J Pharmacol* 144:617–27

Mazzalupo S, Wawersik MJ, Coulombe PA (2002) An *ex vivo* assay to assess the potential of skin keratinocytes for wound epithelialisation. *J Invest Dermatol* 118:866–70

McMillan JR, Akiyama M, Tanaka M, Yamamoto S, Goto M, Abe R *et al.* (2007) Small-diameter porous poly (epsilon-caprolactone) films enhance adhesion and growth of human cultured epidermal keratinocyte and dermal fibroblast cells. *Tissue Eng* 13:789–98

Mildner M, Ballaun C, Stichenwirth M, Bauer R, Gmeiner R, Buchberger M *et al.* (2006) Gene silencing in a human organotypic skin model. *Biochem Biophys Res Commun* 348:76–82

Mori R, Power KT, Wang CM, Martin P, Becker DL (2006) Acute downregulation of connexin43 at wound sites leads to a reduced inflammatory response, enhanced keratinocyte proliferation and wound fibroblast migration. *J Cell Sci* 119:5193–203

Neub A, Houdek P, Ohnemus U, Moll I, Brandner JM (2007) Biphasic regulation of AP-1 subunits during human epidermal wound healing. *J Invest Dermatol* 127:2453–62

Nicholson BJ, Weber PA, Cao F, Chang H, Lampe P, Goldberg G (2000) The molecular basis of selective permeability of connexins is complex and includes both size and charge. *Braz J Med Biol Res* 33:369–78

Parenteau NL, Bilbo P, Nolte CJ, Mason VS, Rosenberg M (1992) The organotypic culture of human skin keratinocytes and fibroblasts to achieve form and function. *Cytotechnology* 9:163–71

Qiu C, Coutinho P, Frank S, Franke S, Law L, Martin P *et al.* (2003) Targeting connexin43 expression accelerates the rate of wound repair. *Curr Biol* 13:1697–703

Richard G, Brown N, Smith LE, Terrinoni A, Melino G, Mackie RM (2000) The spectrum of mutations in erythrokeratodermias-novel and *de novo* mutations in GJB3. *Hum Genet* 106:321–9

Richard G, Rouan F, Willoughby CE, Brown N, Chung P, Ryynanen M *et al.* (2002) Missense mutations in GJB2 encoding connexin-26 cause the ectodermal dysplasia keratitis–ichthyosis–deafness syndrome. *Am J Hum Genet* 70:1341–8

Risek B, Klier FG, Gilula NB (1992) Multiple gap junction genes are utilized during rat skin and hair development. *Development* 116:639–51

Rosdy M, Clauss LC (1990) Terminal epidermal differentiation of human keratinocytes grown in chemically defined medium on inert filter substrates at the air–liquid interface. *J Invest Dermatol* 95:409–14

Salomon D, Masgrau E, Vischer S, Ullrich S, Dupont E, Sappino P *et al.* (1994) Topography of mammalian connexins in human skin. *J Invest Dermatol* 103:240–7

Usui ML, Underwood RA, Mansbridge JN, Muffley, Carter WG, Olerund JE (2005) Morphological evidence for the role of suprabasal keratinocytes in wound reepithelialisation. *Wound Repair Regen* 13: 468–79

Valiunas V, Polosina YY, Miller H, Potapova IA, Valiuniene L, Doronin S *et al.* (2005) Connexin-specific cell-to-cell transfer of short interfering RNA by gap junctions. *J Physiol* 568:459–68

Vreeburg M, de Zwart-Storm EA, Schouten MI, Nellen RG, Marcus-Soekarman D, Devies M *et al.* (2007) Skin changes in oculo-dento-digital dysplasia are correlated with C-terminal truncations of connexin 43. *Am J Med J Genet A* 143:360–3

White TW, Paul DL (1999) Genetic diseases and gene knockouts reveal diverse connexin functions. *Annu Rev Physiol* 61: 283–310

Willecke K, Eiberger J, Degen J, Eckardt D, Romualdi A, Güldenagel M *et al.* (2002) Structural and functional diversity of connexin genes in the mouse and human genome. *Biol Chem* 383:725–37

Wiszniewski L, Limat A, Saurat JH, Meda P, Salomon D (2000) Differential expression of connexins during stratification of human keratinocytes. *J Invest Dermatol* 115:278–85